International Journal of Solids and Structures 47 (2010) 3513–3518

Contents lists available at ScienceDirect

International Journal of Solids and Structures

journal homepage: www.elsevier.com/locate/ijsolstr

Bleustein–Gulyaev waves in 6 mm piezoelectric materials loaded with a viscous liquid layer of finite thickness

Zheng-Hua Qian [a,*], Feng Jin [b], Peng Li [b], Sohichi Hirose [a]

[a] Department of Mechanical and Environmental Informatics, Tokyo Institute of Technology, Tokyo 152-8550, Japan
[b] MOE Key Laboratory for Strength and Vibration, Xi'an Jiaotong University, Xi'an 710049, PR China

ARTICLE INFO

Article history:
Received 1 April 2010
Received in revised form 30 August 2010
Available online 17 September 2010

Keywords:
Bleustein–Gulyaev waves
6 mm piezoelectric materials
Viscous liquid layer of finite thickness
Liquid sensing

ABSTRACT

In this paper, we analyze the propagation of Bleustein–Gulyaev waves in an unbounded piezoelectric half-space loaded with a viscous liquid layer of finite thickness within the linear elastic theories. Exact solutions of the phase velocity equations are obtained in the cases of both electrically open circuit and short circuit by solving the equilibrium equations of piezoelectric materials and the diffusion equation of viscous liquid. A PZT-5H/Glycerin system is selected to perform the numerical calculation. The results show that the mass density and the viscous coefficient have different effects on the propagation attenuation and phase velocity under different electrical boundary conditions. In particular, the penetration depth of the waves is of the same order as the wavelength in the case of electrically short circuit. These effects can be used to manipulate the behavior of the waves and have implications in the application of acoustic wave devices.

1. Introduction

One kind of shear horizontal wave (hereinafter abbreviated to "B–G" wave) can exist along the traction-free surface of piezoelectric materials, which has no counterpart in elastic materials. Following the work by Bleustein (1968) and Gulyaev (1969), many researchers successively investigated the propagation characteristics of the so-called B–G wave in order to apply it to acoustic wave devices (Bleustein, 1969; Li, 1996; Yang, 2000; Liu et al., 2003). Most of the models considered in these works deal with piezoelectric materials. Acoustic wave devices loaded with viscous liquid layers of finite thickness are also widely encountered. For example, it is very common to make an IDT (interdigital transducer) on one side of a piezoelectric crystal, and load viscous liquid on the other side. In this way, the waves transmit less energy into the liquid and keep working at the liquid-loaded circumstance, which works to the traditional surface waves' disadvantage. Kieiczyhskai and Plowiec (1989) made use of the perturbation theory to present a method for measuring the rheological properties of viscoelastic liquids using B–G waves. Because the B–G wave does not radiate energy into the contacting liquid and is sensitive to the changes of liquid density and viscous coefficient, Zhang et al. (2001) proposed that it could be a promising candidate for liquid sensing applications. However, they did not give a detailed quantitative investigation of B–G wave propagation in piezoelectric materials loaded with viscous liquid. Guo and Sun (2008) investigated B–G wave propagation in half-space piezoelectric materials loaded with viscous liquid. The liquid model that Guo et al. adopted in their work is a half-space, which may not be appropriate because the thickness of the liquid layer is much less than that of the piezoelectric substrate. To establish the relationship between shifts in wave frequency and changes in fluid density or viscosity, a coupled problem of fluid–structure interaction using practical solid–liquid models needs to be solved. This usually presents complicated mathematical problems, and only limited theoretical results have been reported so far.

In this paper, we analyze the propagation of B–G waves in an unbounded piezoelectric half-space loaded with a viscous liquid layer of finite thickness. By solving the equilibrium equations of piezoelectric materials and the diffusion equation of viscous liquid, the closed-form solutions for the phase velocity equations of B–G waves are obtained for both the electrically open circuit and short circuit. This analysis is followed by numerical examples of a PZT-5H piezoelectric ceramic half-space in contact with a finite-thickness layer of glycerin. The results obtained in this paper are intended to provide essential data for designing liquid sensing devices.

2. Statement of the problem

Consider a piezoelectric half-space covered with a finite-thickness layer of liquid, as shown in Fig. 1. The ceramic material is

* Corresponding author. Tel./fax: +81 3 5734 2692.
E-mail addresses: qian.z.aa@m.titech.ac.jp, zhenghua_qian@hotmail.com (Z.-H. Qian).

0020-7683/$ - see front matter © 2010 Elsevier Ltd. All rights reserved.
doi:10.1016/j.ijsolstr.2010.08.025

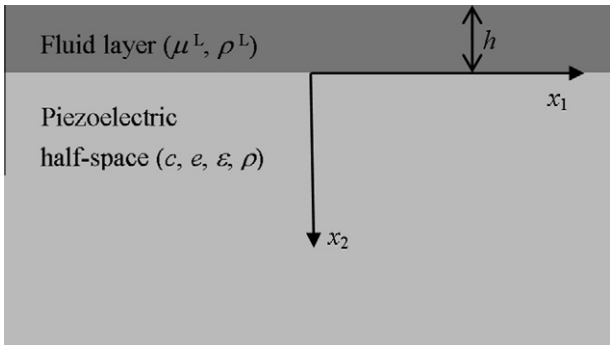

Fig. 1. A piezoelectric half-space covered with a finite-thickness layer of viscous fluid.

poled in the x_3 direction determined by the right-hand rule from the x_1 and x_2 axes. The structure allows the following anti-plane motion (Bleustein, 1969):

$$u_1 = u_2 = 0, \quad u_3 = u(x_1, x_2, t), \tag{1}$$
$$\varphi = \varphi(x_1, x_2, t), \tag{2}$$

where u_1, u_2 and u_3 are the mechanical displacement components and φ is the electric potential. The nontrivial strain and electric field components are

$$\begin{Bmatrix} 2S_{13} \\ 2S_{23} \end{Bmatrix} = \nabla u, \quad \begin{Bmatrix} E_1 \\ E_2 \end{Bmatrix} = -\nabla\varphi, \tag{3}$$

where $\nabla = \mathbf{i}_1\partial_1 + \mathbf{i}_2\partial_2$ is the two-dimensional gradient operator. E_1 and E_2 are the electric field components. The nontrivial components of the stress T_{ij} and the electric displacement D_i in the piezoelectric half-space are

$$\begin{Bmatrix} T_{13} \\ T_{23} \end{Bmatrix} = c\nabla u + e\nabla\varphi, \quad \begin{Bmatrix} D_1 \\ D_2 \end{Bmatrix} = e\nabla u - \varepsilon\nabla\varphi, \tag{4}$$

where we have denoted the relevant elastic, piezoelectric and dielectric constants in the piezoelectric half-space by $c = c_{44}$, $e = e_{15}$ and $\varepsilon = \varepsilon_{11}$. The nontrivial equation of motion and the charge equation of electrostatics take the following forms:

$$\left.\begin{aligned} c\nabla^2 u + e\nabla^2\varphi &= \rho\ddot{u}, \\ e\nabla^2 u - \varepsilon\nabla^2\varphi &= 0, \end{aligned}\right\} \tag{5}$$

for the piezoelectric half-space occupying $0 \leqslant x_2 < +\infty$.

The liquid occupying $-h \leqslant x_2 \leqslant 0$ is assumed to be viscous and nonconductive. Suppose that the motion of liquid is induced only by wave propagation in the piezoelectric material and also propagates in the form of harmonic wave. In this case, the governing equation for the liquid layer is simplified to (Guo and Sun, 2008)

$$\frac{\partial v_3^L}{\partial t} - \frac{\mu^L}{\rho^L}\nabla^2 v_3^L = 0, \tag{6}$$

where v_3^L is the liquid particle velocity along the x_3 direction in the liquid layer. ρ^L is the mass density of the liquid, and μ^L is the dynamic viscous coefficient of the liquid.

The mechanical boundary, continuity and attenuation conditions for the problem under consideration are

$$\begin{aligned} &T_{23}^L = 0 \quad \text{at } x_2 = -h, \\ &T_{23} = T_{23}^L, v_3 = v_3^L \quad \text{at } x_2 = 0, \\ &u_3 \to 0, \varphi \to 0 \quad \text{as } x_2 \to \infty. \end{aligned} \tag{7}$$

Assume that the liquid is electrically insulated and its permittivity is much less than that of the piezoelectric substrate material. The electrical boundary conditions at the solid–liquid interface can thus be classified into two cases, i.e., (1) an electrically open circuit: $D_2|_{x_2=0} = 0$, (2) an electrically short circuit: $\varphi|_{x_2=0} = 0$.

3. Propagating wave solution

The solution of the boundary problem specified in Section 2 can be found in our previous work (Qian et al., 2007, 2009). The solution of Eq. (5) as a plane harmonic wave satisfying the attenuation condition in Eq. (7), is listed directly here:

$$\begin{aligned} u &= C_1 e^{-\xi_2 x_2}\exp[\mathrm{i}(\xi_1 x_1 - \omega t)], \\ \varphi &= \left(C_2 e^{-\xi_1 x_2} + \frac{e}{\varepsilon}C_1 e^{-\xi_2 x_2}\right)\exp[\mathrm{i}(\xi_1 x_1 - \omega t)], \end{aligned} \tag{8}$$

where C_1 and C_2 are undetermined constants, ω is the wave frequency, and ξ_1 and ξ_2 are wave numbers in the x_1 and x_2 directions. Eq. (8) satisfies Eq. (5) when

$$\xi_2^2 = \xi_1^2(1 - v^2/v_T^2), \tag{9}$$

where $\mathrm{Re}(\xi_1) > 0$ and $\mathrm{Re}(\xi_2) > 0$, the wave speed v is given by $\mathrm{Re}(\xi_1) = \omega/v$, $v_T = (\bar{c}/\rho)^{1/2}$ is the bulk shear wave velocity, and $\bar{c} = c + e^2/\varepsilon$ is the piezoelectrically-stiffened elastic constant in the substrate.

Similarly, the solution of Eq. (6) as a plane harmonic wave satisfying the boundary condition at the free surface is written as

$$v_3^L = C_3\cosh\xi_2^L(x_2 + h)\exp[\mathrm{i}(\xi_1 x_1 - \omega t)], \tag{10}$$

where C_3 is an undetermined constant. Eq. (10) satisfies Eq. (6) for

$$\left(\xi_2^L\right)^2 = \xi_1^2 - \mathrm{i}\omega\rho^L/\mu^L. \tag{11}$$

Substitution of Eqs. (8) and (10) and their corresponding stress components into the remaining mechanical boundary and continuity conditions in Eq. (7) yields

$$\begin{aligned} &-\mathrm{i}\omega C_1 = C_3\cosh\xi_2^L h, \\ &-\xi_2\bar{c}C_1 - e\xi_1 C_2 = C_3\mu^L\xi_2^L\sinh\xi_2^L h. \end{aligned} \tag{12}$$

For the electrically open-circuit condition, $C_2 = 0$. For the electrically short-circuit condition, $C_2 + C_1 e/\varepsilon = 0$. For nontrivial solutions of the undetermined constants to exist, the determinant of the coefficient matrix of the linear algebraic equations has to equal zero, which leads to the following dispersion relation of the B–G waves:

$$\xi_2\bar{c} - \mathrm{i}\omega\mu^L\xi_2^L\tanh\xi_2^L h = 0, \tag{13}$$

for an electrically open circuit, and

$$\xi_2\bar{c} - \mathrm{i}\omega\mu^L\xi_2^L\tanh\xi_2^L h - \xi_1 e^2/\varepsilon = 0, \tag{14}$$

for an electrically short circuit.

With Eqs. (9) and (11), we can use Eqs. (13) and (14) to determine v versus ξ_1 or ω versus ξ_1. For the special case when $h \to \infty$, we can separately degenerate Eqs. (13) and (14) into the following:

$$\xi_2\bar{c} - \mathrm{i}\omega\mu^L\xi_2^L = 0, \tag{15}$$
$$\xi_2\bar{c} - \mathrm{i}\omega\mu^L\xi_2^L - \xi_1 e^2/\varepsilon = 0. \tag{16}$$

Eqs. (15) and (16) are exactly the same as the results obtained by Guo and Sun (2008).

4. Numerical examples

We consider a PZT-5H piezoelectric ceramic half-space in contact with a layer of viscous liquid. Material properties of PZT-5H, taken from Fang et al. (2000), are listed as the following:

$$c = 2.3\times10^{10}\ \mathrm{N/m^2}, \quad \rho = 7.5\times10^3\ \mathrm{kg/m^3},$$
$$e = 17.0\ \mathrm{C/m^2}, \quad \varepsilon = 227.0\times10^{-10}\ \mathrm{F/m}.$$

From the work of Bleustein (1968), we can readily know that the B–G wave velocities in the PZT-5H piezoelectric ceramic half-space are v_o = 2182.698 m/s (for open circuit) and v_s = 2039.446 m/s (for short circuit).

For the liquid layer, we select a finite-thickness layer of glycerin. The mass density is $\rho^L = 1.2613 \times 10^3$ kg/m^3 and the viscosity is μ^L = 1.5 Ns/m^2. The electromechanical coupling factor is defined as follows:

$$K^2 = 2\frac{c_{\text{open}} - c_{\text{short}}}{c_{\text{open}}}, \tag{17}$$

where c_{open} and c_{short} are the phase velocities in the cases of electrically open circuit and short circuit, respectively.

4.1. Effect of the liquid thickness

From Eqs. (13) and (14), we can see that B–G wave propagation in this structure is closely related to the thickness of the liquid layer. The results of wave attenuation, velocity and the electromechanical coupling factor with respect to the thickness of the glycerin layer h are shown in Figs. 2–4, respectively. Comparing Fig. 2(a) with Fig. 2(b), we see that attenuation in the case of the electrically short circuit is much larger than that in the case of the electrically open circuit. It can also be seen from Fig. 2 that specific layer thickness show maximum levels of attenuation. From Fig. 4, we can infer that the relationship between the electromechanical coupling factor and the thickness of the glycerin layer is similar to that of attenuation shown in Fig. 2. However, the thickness of the glycerin layer affects the phase velocity in a way different from the attenuation, i.e., there exists a minimum value when the layer thickness changes in the range $0 < h < 8$ μm, as shown in Fig. 3. The attenuation and the phase velocity keep constant when the liquid layer thickness $h > 6$ μm. After considering the effect of the liquid thickness, $h = 2$ μm is adopted for the following analysis.

If the thickness of liquid layer $h \to \infty$ is defined, we can get the same results as Guo and Sun (2008), which illustrates the validity of the phase velocity equations obtained in the current work. On the other hand, when the thickness of the glycerin layer $h = 0$ (i.e., there is no liquid layer, only the piezoelectric ceramic half-space exists), the attenuation will be zero and the phase velocity

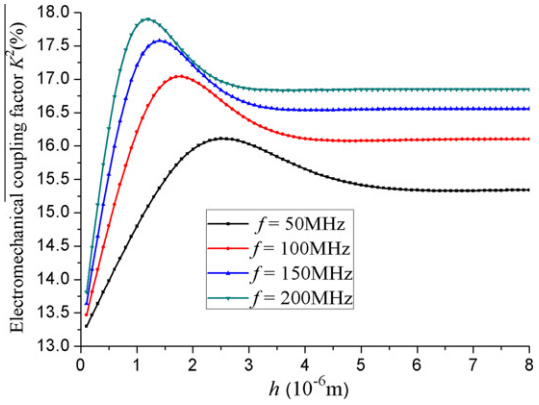

Fig. 4. Electromechanical coupling factor vs. the glycerin layer thickness.

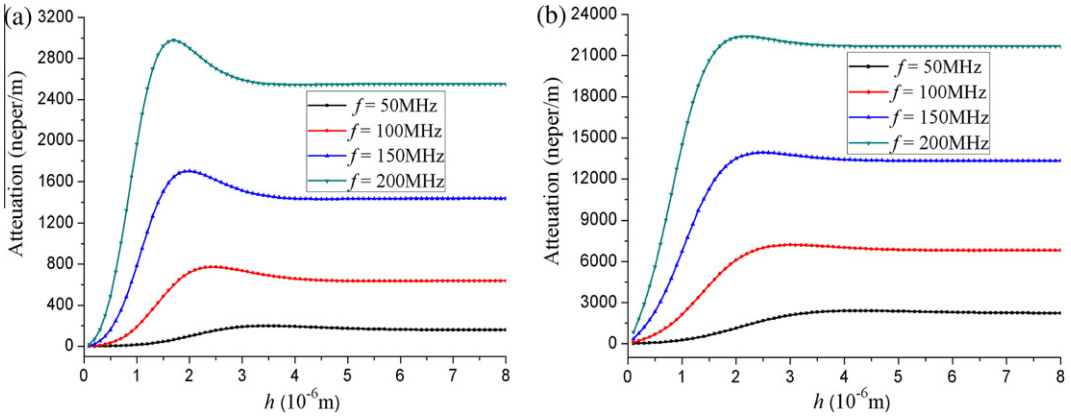

Fig. 2. Attenuation vs. the glycerin layer thickness: (a) electrically open circuit and (b) electrically short circuit.

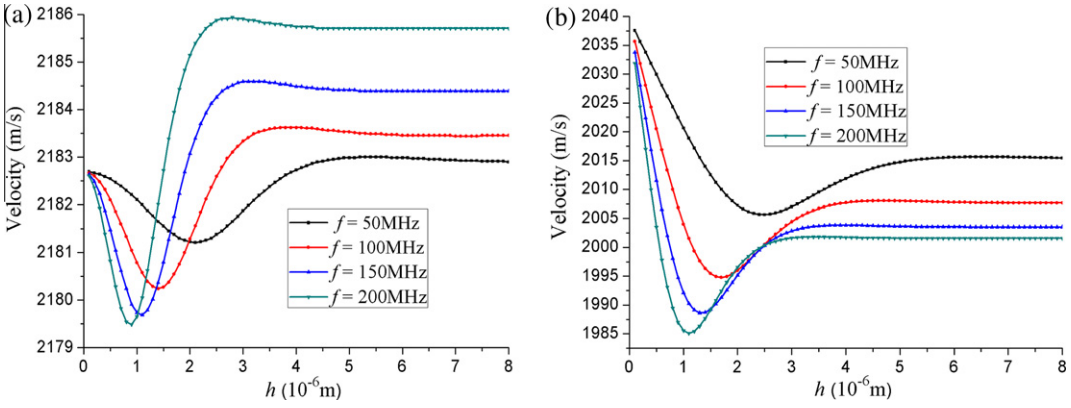

Fig. 3. Phase velocity vs. the glycerin layer thickness: (a) electrically open circuit and (b) electrically short circuit.

will tend to the B–G wave v_o and v_s in a PZT-5H piezoelectric ceramic half-space (Bleustein, 1968), also confirming our calculation to some extent.

4.2. Effect of the mass density and the viscous coefficient

When the external environment changes (such as a rise or drop in temperature), the mass density and the viscous coefficient of the glycerin also change. Because of this, it is important to investigate the propagation of B–G waves when the mass density and the viscous coefficient of the glycerin change. We assume the mass density of glycerin is homogeneous when we focus on the effect of the viscous coefficient, and we assume the viscous coefficient of glycerin is homogeneous when we focus on the effect of the mass density. We define the wave velocity v corresponding to the case when the thickness of glycerin layer $h = 2\ \mu m$, the mass density $\rho^L = 1.2613 \times 10^3\ kg/m^3$ and the viscous coefficient $\mu^L = 1.5\ Ns/m^2$. The velocity corresponding to the case when the mass density or viscous coefficient changes is denoted by v'. Therefore, the nondimensional velocity variation can be defined as $\delta v = (v' - v)/v$. Terms such as δK^2, $\delta\rho^L$, $\delta\mu^L$ and $\delta\mathrm{Im}(\xi_1)$ can be defined similarly. The nondimensional attenuation variation $\delta\mathrm{Im}(\xi_1)$, the nondimensional velocity variation δv and the nondimensional electromechanical coupling factor variation δK^2 are plotted separately in Figs. 5–9 for selected values of frequency when the glycerin viscosity $\delta\mu^L$ and mass density $\delta\rho^L$ change from −50% to 50%, respectively.

It can be readily seen from Fig. 5 that the relationship between the attenuation variation $\delta\mathrm{Im}(\xi_1)$ and the glycerin viscosity variation $\delta\mu^L$ is nonlinear no matter if the electrical condition is open circuit or short circuit. In addition, the case of frequency $f = 50$ MHz presents a completely different pattern from that for the other three frequency values. For $f = 50$ MHz, with the increase of the glycerin viscosity in the case of electrically open circuit, the attenuation variation $\delta\mathrm{Im}(\xi_1)$ increases at first, and then decreases slowly (shown in Fig. 5(a); while in the case of electrically short circuit, the attenuation variation $\delta\mathrm{Im}(\xi_1)$ decreases monotonously with the increase of the glycerin viscosity (shown in Fig. 5(b). From Fig. 6, we can see that the attenuation variation increases almost linearly with the increase of the mass density except for the case when $f = 50$ MHz, regardless of the electrical conditions. From a comparison between Fig. 5(a) and (b) and between Fig. 6(a) and (b), we can see that the attenuation variation caused by a change of the mass density is larger than that caused by a change of the glycerin viscosity. Moreover, from the comparison between Figs. 5 and 6, we can also see that the attenuation variation in the case of electrically open circuit is larger than in the case of electrically short circuit.

Figs. 7 and 8 present the variation patterns of nondimensional velocity δv as a function of viscosity variation $\delta\mu^L$ and mass density

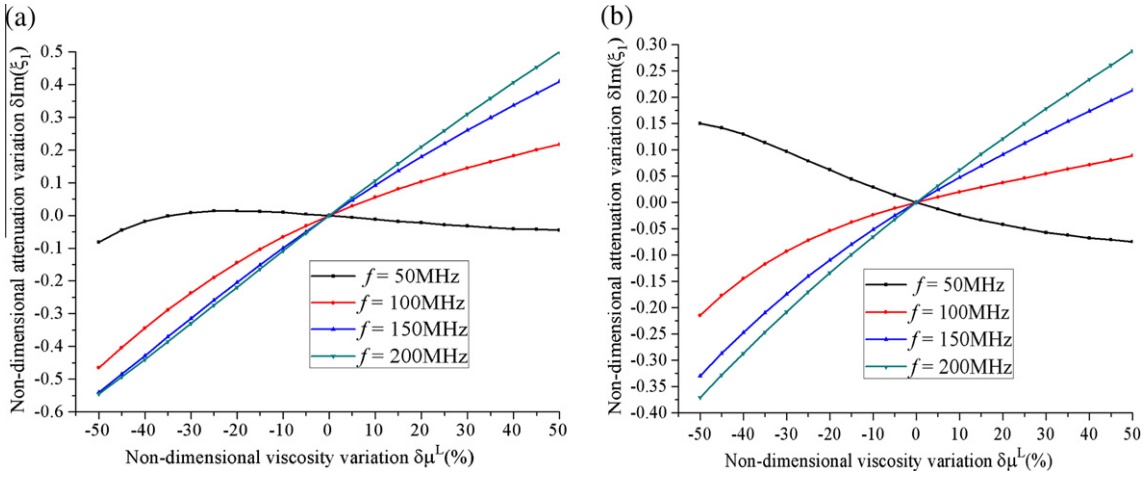

Fig. 5. Variation of nondimensional attenuation $\delta\mathrm{Im}(\xi_1)$ vs. $\delta\mu^L$: (a) electrically open circuit and (b) electrically short circuit.

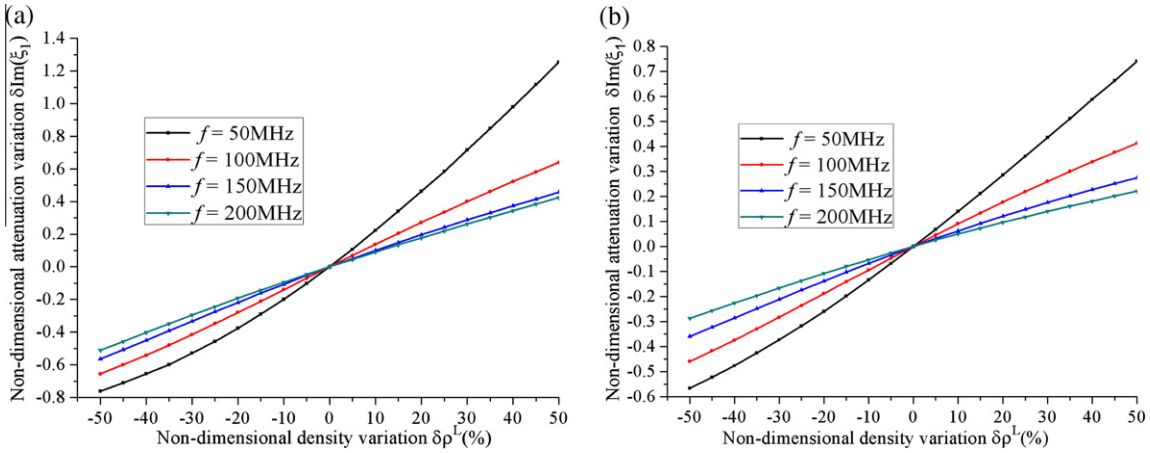

Fig. 6. Variation of nondimensional attenuation $\delta\mathrm{Im}(\xi_1)$ vs. $\delta\rho^L$: (a) electrically open circuit and (b) electrically short circuit.

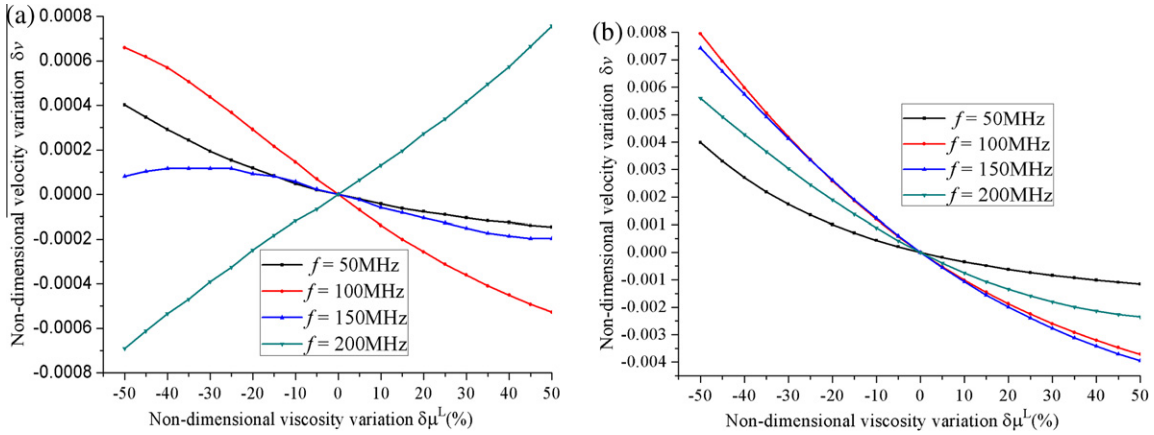

Fig. 7. Variation of nondimensional velocity δv vs. $\delta\mu^L$: (a) electrically open circuit and (b) electrically short circuit.

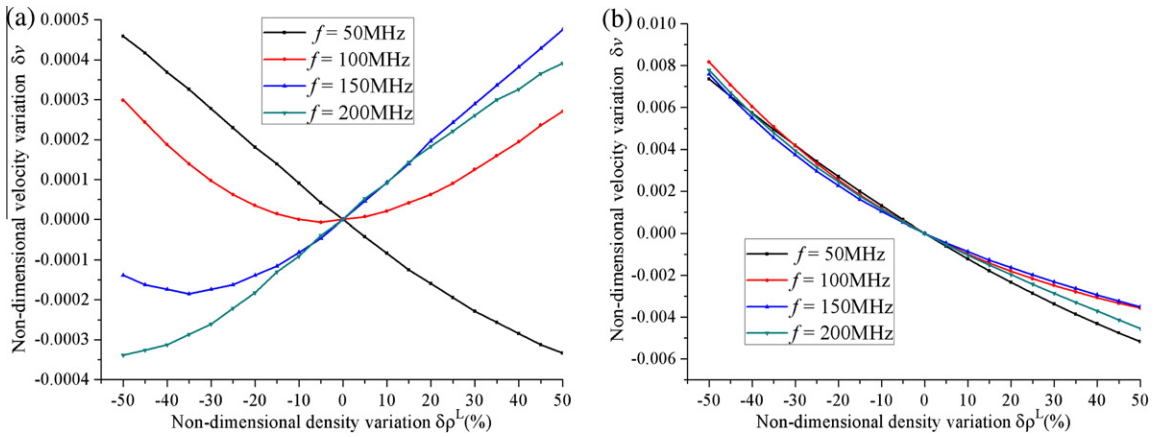

Fig. 8. Variation of nondimensional velocity δv vs. $\delta\rho^L$: (a) electrically open circuit and (b) electrically short circuit.

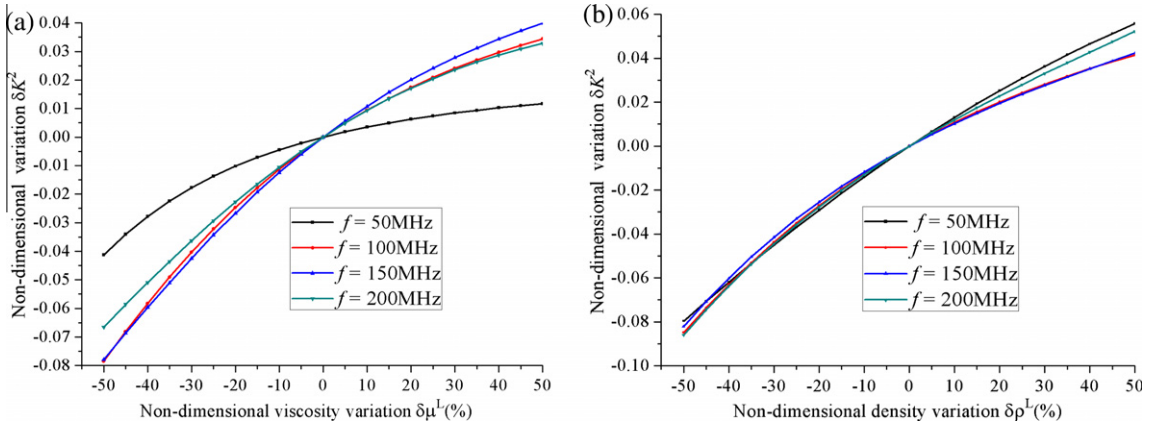

Fig. 9. Variation of nondimensional electromechanical coupling factor δK^2 as a function of: (a) viscosity variation $\delta\mu^L$ and (b) mass density variation $\delta\rho^L$.

variation $\delta\rho^L$ for selected values of frequency. It can be seen from Fig. 7 that the variation patterns of δv vs. $\delta\mu^L$ for different frequency values differ from each other very much in the case of electrically open circuit. In the case of electrically short circuit, δv decreases with the increase of $\delta\mu^L$ for all of the selected frequency values. Phenomena similar these exist in the variation patterns of δv vs. $\delta\rho^L$ for different frequency values, as shown in Fig. 8. However, the frequency in the latter has negligible influence on the variation of δv vs. $\delta\rho^L$ in the case of the electrically short circuit. Further observation of Figs. 7 and 8 reveals that the total change of nondimensional velocity δv in the case of the electrically open circuit is less than one tenth of that in the case of the electrically short circuit.

Fig. 9 shows the variation of the nondimensional electromechanical coupling factor δK^2 as a function of the viscosity variation $\delta\mu^L$ and the mass density variation $\delta\rho^L$ for selected values of frequency. The electromechanical coupling factor variation δK^2 increases with the increase of the viscous coefficient or the mass

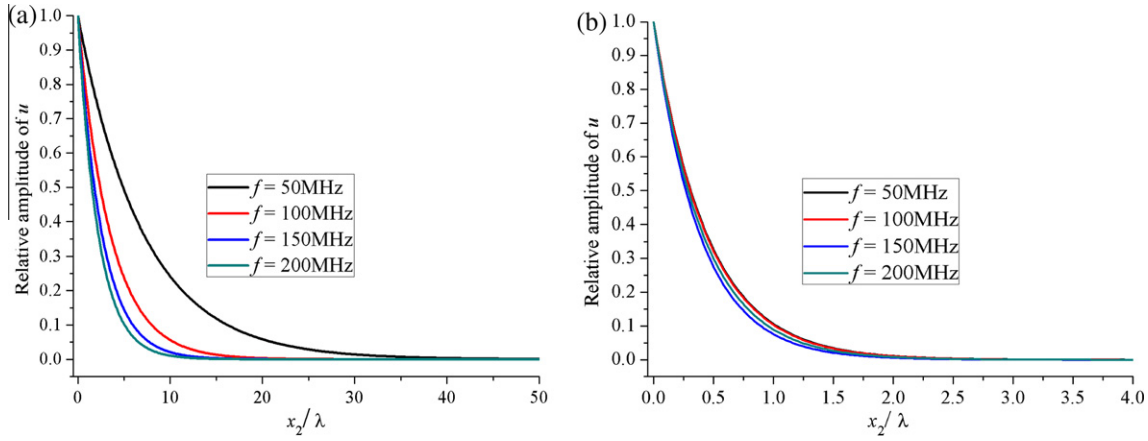

Fig. 10. Distribution of mechanical displacement in the piezoelectric half-space with the glycerin layer: (a) electrically open circuit and (b) electrically short circuit.

density, regardless of the frequency value. The frequency value can speed up or slow down the change of electromechanical coupling factor in the case of the electrically open circuit. In the case of the electrically short circuit, however, the frequency value has a negligible effect on this change.

4.3. Penetration depth

Fig. 10 gives the distribution of the relative amplitude of the mechanical displacement u in the piezoelectric substrate for selected frequency values. The mechanical displacement tends to zero within two wavelengths in the case of the electrically short circuit, while in the case of electrically open circuit the mechanical displacement does not approach zero until several tens of wavelengths. This means the penetration depth in the case of electrically open circuit is much greater than in the case of electrically short circuit. It can also be seen that the penetration depth does not significantly change for different frequency values in the case of electrically short circuit (shown in Fig. 10(b). In the case of electrically open circuit (shown in Fig. 10(a), the frequency value has an important effect on the penetration depth. Specifically, low frequency waves have larger penetration depth and high frequency waves have smaller penetration depth. This observation agrees with physical intuition, validating the correctness of our calculation to some extent.

5. Conclusions

In this paper, we studied the propagation of B–G waves in a piezoelectric half-space of 6 mm symmetry in contact with a viscous liquid layer of finite thickness. The explicit dispersion relations in the cases of both an electrically open circuit and a short circuit are obtained analytically. A numerical example is calculated for a PZT-5H piezoelectric ceramic loaded with a finite-thickness glycerin layer. Some conclusions are drawn below:

(1) A change of the attenuation and velocity is evident when the thickness of the glycerin layer changes within the range $0 < h < 6$ μm, while the effect of the thickness of the liquid layer on the change of phase velocity and attenuation of B–G waves is negligible for $h > 6$ μm.
(2) The relationship between attenuation and viscosity is nonlinear, while the relationship between attenuation and the mass density is approximately linear except for the case of $f = 50$ MHz for both electrically open and short circuits. Moreover, the effect of mass density on attenuation is larger than that of viscosity.
(3) The penetration depth in the case of an electrically open circuit is much greater than in the case of an electrically short circuit. Specifically, the penetration depth of B–G waves is on the same order as the wavelength in the case of the electrically short circuit.

The results reported in this paper can be used as a benchmark for further investigation of wave propagation in piezoelectric coupled structures, and it is also theoretically significant to the design of wave propagation in piezoelectric coupled structures loaded with viscous liquid layers of finite thickness.

Acknowledgements

The author (Z.H. Qian) gratefully acknowledges the support of the Global COE Program at the Tokyo Institute of Technology. One of the authors (F. Jin) gratefully acknowledges the support of the National Natural Science Foundation of China (No. 10972171) and the Program for New Century Excellent Talents in Universities (No. NCET-08-0429).

References

Bleustein, J.L., 1968. A new surface wave in piezoelectric materials. Appl. Phys. Lett. 13, 412–413.
Bleustein, J.L., 1969. Some simple modes of wave propagation in an infinite piezoelectric plate. J. Acoust. Soc. Am. 45, 614–620.
Fang, H.Y., Yang, J.S., Jiang, Q., 2000. Rotation-perturbed surface acoustic waves propagating in piezoelectric crystals. Int. J. Solids Struct. 37, 4933–4947.
Gulyaev, Y.V., 1969. Electroacoustic surface waves in solids. JETP Lett. 9, 37–38.
Guo, F.L., Sun, R., 2008. Propagation of Bleustein–Gulyaev wave in 6mm piezoelectric materials loaded with viscous liquid. Int. J. Solids Struct. 45, 3699–3710.
Kieiczyhskai, P., Plowiec, R., 1989. Determination of the shear impedance of viscoelastic liquids using Love and Bleustein–Gulyaev surface waves. J. Acoust. Soc. Am. 86, 818–827.
Li, S.F., 1996. The electromagneto-acoustic surface wave in a piezoelectric medium: the Bleustein–Gulyaev mode. J. Appl. Phys. 80, 5264–5269.
Liu, H., Kuang, Z.B., Cai, Z.M., 2003. Propagation of Bleustein–Gulyaev waves in a prestressed layered piezoelectric structure. Ultrasonics 41, 397–405.
Qian, Z., Jin, F., Lu, T., Kishimoto, K., 2009. Transverse surface waves in a layered structure with a functionally graded piezoelectric substrate and a hard dielectric layer. Ultrasonics 49, 293–297.
Qian, Z., Jin, F., Wang, Z., Kishimoto, K., 2007. Transverse surface waves on a piezoelectric material carrying a functionally graded layer of finite thickness. Int. J. Eng. Sci. 45, 455–466.
Yang, J.S., 2000. Bleustein–Gulyaev waves in piezoelectromagnetic materials. Int. J. Appl. Electromagnet Mech. 12, 235–240.
Zhang, C., Caron, J.J., Vetelino, J.F., 2001. The Bleustein–Gulyaev wave sensing application. Sens. Actuators B Chem. 76, 64–68.